J|A|C|S ARTICLES

Published on Web 09/28/2009

# Managing Highly Coordinative Substrates in Asymmetric Catalysis: A Catalytic Asymmetric Amination with a Lanthanum-Based Ternary Catalyst

Tomoyuki Mashiko, Naoya Kumagai,* and Masakatsu Shibasaki*

*Graduate School of Pharmaceutical Sciences, The University of Tokyo, 7-3-1 Hongo, Bunkyo-ku, Tokyo, 113-0033, Japan*

Received June 26, 2009; E-mail: mshibasa@mol.f.u-tokyo.ac.jp; nkumagai@mol.f.u-tokyo.ac.jp

***Abstract:*** Full details of a catalytic asymmetric amination with a lanthanum/amide-based ligand catalyst system are described. A catalyst comprising $La(NO_3)_3 \bullet 6H_2O$, (*R*)-**3a** and H-D-Val-O$^t$Bu was identified to promote the catalytic asymmetric amination of nonprotected succinimide derivative **1** with as little as 1 mol % catalyst loading. Mechanistic studies by various spectroscopic analyses and several control and kinetic experiments suggested that the catalyst components were in equilibrium between the associated and dissociated forms, and that the reaction likely proceeded through a $La(NO_3)_3 \bullet 6H_2O$/(*R*)-**3a**/H-D-Val-O$^t$Bu ternary complex. This catalyst system was also effective for asymmetric amination of *N*-nonsubstituted α-alkoxycarbonyl amides **7**, hitherto unprecedented substrates in asymmetric catalysis, probably due to their attenuated reactivity and difficult stereocontrol, affording the amination products in up to >99% yield and >99% ee. The high catalytic performance and enantiocontrol of the reaction with highly coordinative substrates were achieved by the activation/recognition of the substrates exerted by coordination to lanthanum and hydrogen bonding cooperatively in the transition state.

## Introduction

Nitrogen-containing substructures in which nitrogen is directly attached to a stereogenic carbon are a common structural motif in a wide variety of biologically active compounds and therapeutics.[1] Recent advances in asymmetric catalysis have enabled the enantioselective construction of this class of substructures. Because of the nucleophilic character of nitrogen, the majority of strategies involve the enantioselective formation of a C−N bond with a nitrogen-based nucleophile or C═N bond formation followed by enantioselective addition to the C═N bond.[2] Alternatively, electrophilic amination using formal "$NH_2^+$" reagents constitutes a complementary methodology, which allows the installation of a nitrogen functionality adjacent to a carbonyl group.[3] Among the amination reagents used, azodicarboxylates have gained popularity due to their commercial availability and high electrophilic nature.[4] Although the utility of azodicarboxylates in electrophilic amination of carbonyl compounds was reported in 1954,[5] only recently has this same transformation been rendered asymmetric using a magnesium bis(sulfonamide) catalyst.[6] Several catalytic asymmetric electrophilic aminations of carbonyl compounds have been successively reported with both metal-based catalysts and organocatalysts.[7−9]

We were particularly interested in the catalytic asymmetric amination of nonprotected succinimide derivative **1**, which

(1) (a) Genet, J.-P., Greck, C.; Lavergne, D. In *Modern Amination Methods*; Ricci, A., Ed.; Wiley-VCH: Weinheim, 2000; chapter 3. (b) Krohn, K. In *Organic Synthesis Highlights*; Wiley-VCH: Weinheim, 1991; pp 45−53.

(2) For selected reviews on catalytic asymmetric addition to C═N double bond, see: (a) Friestad, G. K.; Mathies, A. K. *Tetrahedron* **2007**, *63*, 2541. (b) Weinreb, S. M.; Orr, R. K. *Synthesis* **2005**, 1205. (c) Marques, M. M. B. *Angew. Chem., Int. Ed.* **2006**, *45*, 348. (d) Ting, A.; Schaus, S. E. *Eur. J. Org. Chem.* **2007**, 5797. (e) Verkade, J. M. M.; van Hemert, L. J. C.; Quaedflieg, P. J. L. M.; Rutjes, F. P. J. T. *Chem. Soc. Rev.* **2008**, *37*, 29. For a general review on catalytic asymmetric Mannich reactions, see: (f) Kobayashi, S.; Ueno, M. In *Comprehensive Asymmetric Catalysis, Supplement 1*; Jacobsen, E. N., Pfaltz, A., Yamamoto, H., Eds.; Springer: Berlin, 2004; pp 143−150 (chap 29.5).

(3) For reviews, see: (a) Genet, J. P.; Greck, C. *Synlett* **1997**, 741. (b) Erdik, E. *Tetrahedron* **2004**, *60*, 8747.

(4) For a general review of the use of azodicarboxylates in C−N bond-forming reactions, see: (a) Nair, V.; Biju, A. T.; Mathew, S. C.; Babu, B. P. *Chem. Asian J.* **2008**, *3*, 810.

(5) (a) Huisgen, R.; Jakob, F *Justus Liebigs Ann. Chem.* **1954**, *590*, 37. For electrophilic amination using azodicarboxylates, see: (b) Diels, O *Justus Liebigs Ann. Chem.* **1922**, *429*, 1. (c) Diels, O.; Behncke, H. *Chem. Ber.* **1924**, *57*, 653.

(6) (a) Evans, D. A.; Nelson, S. G. *J. Am. Chem. Soc.* **1997**, *119*, 6452. (b) Evans, D. A.; Johnson, D. S. *Org. Lett.* **1999**, *1*, 595.

(7) For reviews of catalytic asymmetric electrophilic amination of carbonyl compounds, see: (a) Duthaler, R. O. *Angew. Chem., Int. Ed.* **2003**, *42*, 975. (b) Greck, C; Drouillat, B.; Thomassigny, C. *Eur. J. Org. Chem.* **2004**, 1377. (c) Janey, J. M. *Angew. Chem., Int. Ed.* **2005**, *44*, 4292. (d) Cativiela, C.; Ordóñez, M. *Tetrahedron: Asymmetry* **2009**, *20*, 1.

(8) For selected examples using metal-based catalysts, see: (a) Marigo, M.; Juhl, K.; Jørgensen, K. A. *Angew. Chem., Int. Ed.* **2003**, *42*, 1367. (b) Ma, S.; Jiao, N.; Zheng, Z.; Ma, Z.; Lu, Z.; Ye, L.; Deng, Y.; Chen, G. *Org. Lett.* **2004**, *6*, 2193. (c) Foltz, C.; Stecker, B.; Marconi, G.; Bellemin-Laponnaz, S.; Wadepohl, H.; Gabe, L. H. *Chem. Commun.* **2005**, 5115. (d) Bernardi, L.; Zhuang, W.; Jørgensen, K. A. *J. Am. Chem. Soc.* **2005**, *127*, 5772. (e) Kim, Y. K.; Kim, D. Y. *Tetrahedron Lett.* **2006**, *47*, 4565. (f) Comelles, J.; Pericas, A.; Moreno-Mañas, M.; Vallribera, A.; Drudis-Solé, G.; Lledos, A.; Parella, T.; Roglans, A.; García-Granda, S.; Roces-Fernández, L. *J. Org. Chem.* **2007**, *72*, 2077. (g) Hasegawa, Y.; Watanabe, M.; Gridnev, I. D.; Ikariya, T. *J. Am. Chem. Soc.* **2008**, *130*, 2158. (h) Mang, J. Y.; Kwon, D. G.; Kim, D. Y. *J. Fluorine Chem.* **2009**, *130*, 259. (i) Ikariya, T.; Gridnev, I. D. *Chem. Record.* **2009**, *9*, 106.



**10.1021/ja9052653 CCC: $40.75** 

***Scheme 1.*** Concise Enantioselective Synthesis of (−)-**2**

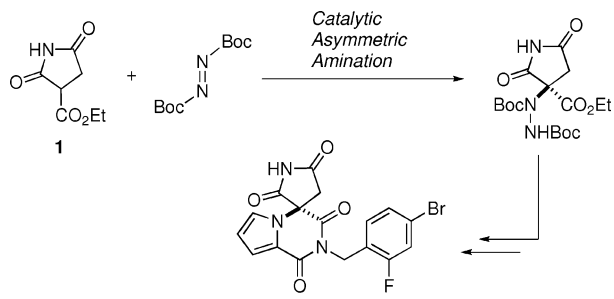


allows for an efficient enantioselective synthesis of AS-3201((−)-**2**, ranirestat), a highly potent aldose reductase inhibitor (Scheme 1). (−)-**2** has attracted particular attention because of its effectiveness for treating diabetic complications via oral administration.[10] Diabetes is one of the most serious health concerns throughout the world, and the number of patients with diabetes is rapidly increasing.[11] The main focus in the treatment of diabetes is on decreasing blood glucose levels, and there are few effective therapeutics for the treatment of late-stage pathologic conditions that seriously compromise patients' quality of life.[12] Clinical trials on (−)-**2** specifically for diabetic neuropathy are ongoing, and therapeutic development is highly anticipated. In this context, an efficient route for the enantioselective synthesis of (−)-**2** is in high demand to fulfill a prospective future supply. Catalytic asymmetric amination of succinimide derivative **1** emerged as a primary option toward this end. The Lewis basicity of nonprotected **1**, however, interferes with the efficient enantiodifferentiation by Lewis acidic chiral catalysts, likely because of the multiple coordination modes displayed by **1**.[13] To address this issue, we initiated studies aimed at developing a catalytic asymmetric amination of **1**.[14,15] We recently achieved a concise enantioselective synthesis of (−)-**2**, in which the catalytic asymmetric amination of **1** with a lanthanum/amide-based ligand catalyst was a key step.[14,16,17] The amination reaction was scalable, cost-effective, and the investigations of an industrial application are underway.[14b] This article describes the full details of the catalytic asymmetric amination with the La/amide-based ligand catalyst system. Based on analyses of the privileged functional group arrangement of the highly coordinative substrates, the substrate scope was successfully expanded to other nonprotected substrates, such as *N*-nonsubstituted α-alkoxycarbonyl amides. Mechanistic studies suggested that the three components of the second-generation catalyst were in a dynamic equilibrium and an associated ternary complex was involved in the transition state.

## Results and Discussion

**Development of the First-Generation Amination Catalyst.** Our initial effort was devoted to the development of a new class of catalysts for catalytic asymmetric amination of nonprotected, highly coordinative succinimide derivative **1**. To avoid ligand dissociation and/or a multiple coordination pattern of **1**, we initially focused on an asymmetric catalyst comprising a rare earth metal (RE)/amide-based ligand, where the high affinity of the amide functionality to RE would avoid ligand dissociation by **1**. Taking high coordination number of REs into account, **1** could coordinate to REs surrounded by amide-based ligands and the hydrogen bonding provided by the ligand could specify the coordination mode of **1**. Three types of amide-based ligands bearing a phenol functionality for coordination to RE, salicylic acid-type (*S*)-**3**, biphenol-type (*S*)-**4**, and hydroxamic acid-type (*S*)-**5**, were examined in the catalytic asymmetric amination of **1** and di-*t*-butyl azodicarboxylate (Scheme 2). The catalyst was prepared by mixing the ligand and La(O$^i$Pr)$_3$ in a 2:1 ratio. The catalyst prepared from ligands (*S*)-**3a**-**d** or (*S*)-**4** efficiently promoted the desired reaction at −40 °C to give (+)-**6**, whereas the catalyst prepared from (*S*)-**5** failed the reaction, presumably because the strongly coordinative hydroxamic acid induced the formation of a catalytically inactive aggregate. The reaction with (*S*)-**3a** gave the highest enantioselectivity, and further investigation revealed that lanthanum worked best among the REs tested,

(9) For selected examples using organocatalysts, see: (a) Sabby, S.; Bella, M.; Jørgensen, K. A. *J. Am. Chem. Soc.* **2004**, *126*, 8120. (b) Pihko, P. M.; Pohjakallio, A. *Synlett* **2004**, 2115. (c) Liu, X.; Li, X.; Deng, L. *Org. Lett.* **2005**, *7*, 167. (d) Xu, X.; Yabuta, T.; Yuan, P.; Takemoto, Y. *Synlett* **2006**, 137. (e) Terada, M.; Nakano, M.; Ube, H. *J. Am. Chem. Soc.* **2006**, *128*, 16044. (f) Liu, Y.; Melgar-Fernandez, R.; Juaristi, E. *J. Org. Chem.* **2007**, *72*, 1522. (g) Jung, S. H.; Kim, D. Y. *Tetrahedron Lett.* **2008**, *49*, 5527. (h) He, R.; Wang, X.; Hashimoto, T.; Maruoka, K. *Angew. Chem., Int. Ed.* **2008**, *47*, 9466. (i) Lan, Q.; Wang, X.; He, R.; Ding, C.; Maruoka, K. *Tetrahedron Lett.* **2009**, *50*, 3280. (j) Liu, X.; Sun, B.; Deng, L. *Synlett* **2009**, *10*, 1685. (k) Cheng, L.; Liu, L.; Wang, D.; Chen, Y.-J. *Org. Lett.* **2009**, *11*, 3874.

(10) (a) Negoro, T.; Murata, M.; Ueda, S.; Fujitani, B.; Ono, Y.; Kuromiya, A.; Komiya, M.; Suzuki, K.; Matsumoto, J.-I. *J. Med. Chem.* **1998**, *41*, 4118. (b) Kurono, M.; Fujiwara, I.; Yoshida, K. *Biochemistry* **2001**, *40*, 8216. (c) Bril, V.; Buchanan, R. A. *Diabetes Care* **2004**, *27*, 2369. (d) Kurono, M.; Fujii, A.; Murata, M.; Fujitani, B.; Negoro, T. *Biochem. Pharmacol.* **2006**, *71*, 338. (e) Giannoukakis, N. *Curr. Opin. Investig. Drugs* **2006**, *7*, 916. (f) Matsumoto, T.; Ono, Y.; Kurono, M.; Kuromiya, A.; Nakamura, K.; Bril, V. *J. Pharmacol. Sci.* **2008**, *107*, 231.

(11) (a) Nath, D.; Heemels, M.-T.; Anson, L. *Nature* **2006**, *444*, 839. and the following review articles. (b) International Diabetes Federation (IDF), Diabetes Atlas, 3rd Edition, Dec, 2006; http://www.iotf.org/diabetes.asp.

(12) For selected examples of the studies toward the treatment of diabetic complications: Selective PKC $\beta$2 inhibitor for the treatment of diabetic neuropathy, see: (a) Inoguchi, T.; Battan, R.; Handler, E.; Sportsman, J. R.; Heath, W.; King, G. L. *Proc. Natl. Acad. Sci. U.S.A.* **1992**, *89*, 11059. (b) Ishii, H.; Jirousek, M. R.; Koya, D.; Takagi, C.; Xia, P.; Clermont, A.; Bursell, S.-E.; Kern, T. S.; Ballas, L. M.; Heath, W. F.; Stramm, L. E.; Feener, E. P.; King, G. L. *Science* **1996**, *272*, 728. (c) Tanaka, M.; Sagawa, S.; Hoshi, J.-I.; Shimoma, F.; Yasue, K.; Ubukata, M.; Ikemoto, T.; Hase, Y.; Takahashi, M.; Sasase, T.; Ueda, N.; Matsushita, M.; Inaba, T. *Bioorg. Med. Chem.* **2006**, *14*, 5781, and references cited therein. Inhibition of vascular endothelial growth factor (VEGF) for prevention of diabetic microvascular complications, see: (d) Gemma, T.; Rosangela, L.; Gabriella, M.; Gianpaolo, Z. *Am. J. Cardiovasc. Drugs* **2007**, *7*, 393.

(13) Representative metal catalysts (Cu-BOX, LaPyBox) and organocatalysts (chiral urea catalyst, cinchona alkaloids) afforded the desired product in less than 30% ee (see ref 14a).

(14) (a) Mashiko, T.; Hara, K.; Tanaka, D.; Fujiwara, Y.; Kumagai, N.; Shibasaki, M. *J. Am. Chem. Soc.* **2007**, *129*, 11342. (b) Mashiko, T.; Kumagai, N.; Shibasaki, M. *Org. Lett.* **2008**, *10*, 2725.

(15) Catalytic asymmetric amination of *N*-Boc protected **1** was reported in refs 9h and 9i.

(16) Other examples of asymmetric catalysis using rare earth metal/amide-based ligand catalysts, see: (a) Nishida, A.; Yamanaka, M.; Nakagawa, M. *Tetrahedron Lett.* **1999**, *40*, 1555. (b) Nitabaru, T.; Kumagai, N.; Shibasaki, M. *Tetrahedron Lett.* **2008**, *49*, 272. (c) Sudo, Y.; Shirasaki, D.; Harada, S.; Nishida, A. *J. Am. Chem. Soc.* **2008**, *130*, 12588. (d) Nojiri, A.; Kumagai, N.; Shibasaki, M. *J. Am. Chem. Soc.* **2008**, *130*, 5630. (e) Nojiri, A.; Kumagai, N.; Shibasaki, M. *J. Am. Chem. Soc.* **2009**, *131*, 3779.

(17) For recent selected examples of small peptide-based asymmetric catalysis, see: (a) Zhao, Y.; Rodrigo, J.; Hoveyda, A. H.; Snapper, M. C. *Nature* **2006**, *443*, 67. (b) Lewis, C. A.; Chiu, A.; Kubryk, M.; Balsells, J.; Pollard, D.; Esser, C. K.; Murry, J.; Reamer, R. A.; Hansen, K. B.; Miller, S. J. *J. Am. Chem. Soc.* **2006**, *128*, 16454. For reviews, see: (c) Hoveyda, A. H.; Hird, A. W.; Kacprzynski, M. A. *Chem. Commun.* **2004**, 1779. (d) Blank, J. T.; Miller, S. J. *Biopolymers (Pept. Sci.)* **2006**, *84*, 38.

***Scheme 2.*** Catalytic Asymmetric Amination of La/Amide-Based Ligand Catalyst

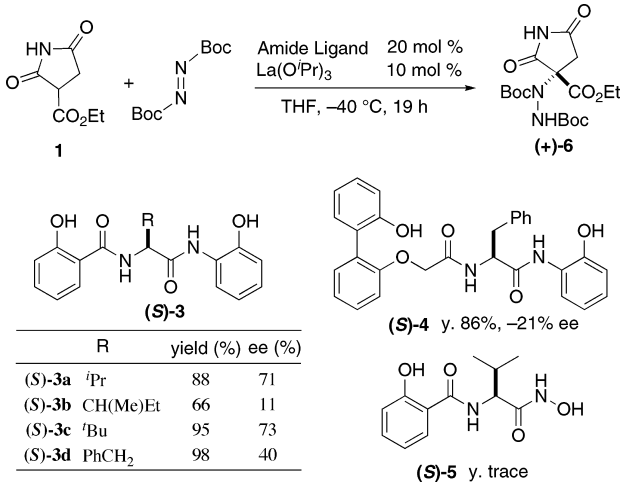


| | R | yield (%) | ee (%) |
|---|---|---|---|
| (*S*)-**3a** | $^i$Pr | 88 | 71 |
| (*S*)-**3b** | CH(Me)Et | 66 | 11 |
| (*S*)-**3c** | $^t$Bu | 95 | 73 |
| (*S*)-**3d** | PhCH$_2$ | 98 | 40 |

***Scheme 3.*** First-Generation Amination Catalyst

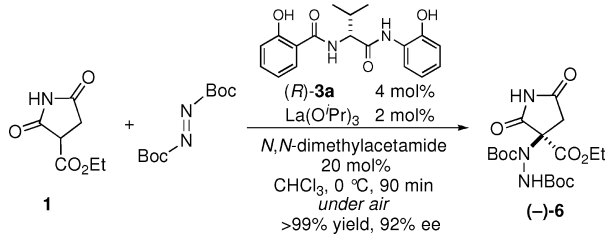


and $CHCl_3$ solvent in the presence of *N*,*N*-dimethylacetamide (DMA) was optimum, establishing a first-generation catalyst.[14a] With 2 mol % catalyst, the asymmetric amination proceeded smoothly at 0 °C under air to furnish amination product (−)-**6** in >99% yield and 92% ee (Scheme 3). (*R*)-**3a** was readily synthesized from Boc-D-valine in high yield via a 5-pot sequence without chromatographic purification. Compound (−)-**6** was successfully converted to (−)-**2** in an optically pure form after a 5-step transformation and a single recrystallization.[10a,14a,18]

**Development of the Second-Generation Catalyst.** Although the first-generation catalyst provided the amination product in 92% ee under air, several concerns remained in regard to the industrial application; (1) La(O$^i$Pr)$_3$ is costly ($224/3 g, Aldrich)[19] and not available in bulk quantities; (2) La(O$^i$Pr)$_3$ is unstable to moisture and must be handled in an inert atmosphere; (3) fluctuation in both reactivity and enantioselectivity was occasionally observed depending on the production lot of La(O$^i$Pr)$_3$; and (4) the use of halogenated solvent ($CHCl_3$) is undesired. To address these issues, we began to search for a more appropriate lanthanum source (Table 1). In contrast to the basic nature of La(O$^i$Pr)$_3$, the readily available lanthanum salts shown in Table 1 are neutral and required an additional base to promote the amination of **1**. The amination reaction was performed with a catalyst prepared from La salt/(*R*)-**3a**/KO$^t$Bu in a 1:2:3 ratio using AcOEt as the solvent, which is less toxic than a halogenated solvent and more favorable for industrial implementation. When 10 mol % of $LaCl_3$ was used, the reaction mixture was heterogeneous due to the poor solubility of $LaCl_3$

***Table 1.*** Screening of Several La Salts[a]

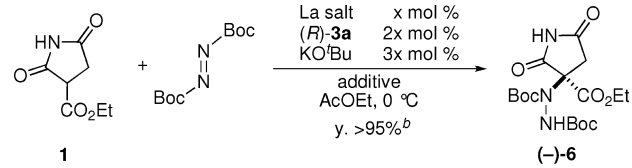


| entry | La salt | x | additive (30 mol %) | time (h) | ee (%) |
|---|---|---|---|---|---|
| 1 | $LaCl_3$ | 10 | – | 0.5 | −2 |
| 2[c] | $LaCl_3$ | 10 | – | 0.5 | 29 |
| 3 | $LaBr_3$ | 10 | – | 4 | 83 |
| 4[d] | $LaBr_3$ | 2.5 | – | 0.75 | 23 |
| 5 | $LaI_3$ | 10 | – | 1 | 14 |
| 6 | La(OTf)$_3$ | 10 | – | 1 | 11 |
| 7 | $LaCl_3$ | 10 | $^n$Bu$_4$N(NO$_3$) | 4.5 | 82 |
| 8 | $LaCl_3$ | 10 | NH$_4$(NO$_3$) | 10 | 67 |
| 9 | La(NO$_3$)$_3$·6H$_2$O | 10 | – | 4 | 68 |
| 10[d] | La(NO$_3$)$_3$·6H$_2$O | 2.5 | – | 3 | 58 |

[a] **1**: 0.2 mmol, BocN=NBoc: 0.24 mmol. [b] Determined by $^1$H NMR analysis with $Bn_2O$ as an internal standard. [c] $LaCl_3$ and KO$^t$Bu were stirred at 50 °C for 30 min. [d] **1**: 0.4 mmol, BocN=NBoc: 0.48 mmol.

and (−)-**6** was obtained in a nearly racemic form (entry 1). Stirring the $LaCl_3$/KO$^t$Bu mixture at 50 °C before adding the (*R*)-**3a** marginally improved the enantioselectivity (entry 2). Among other lanthanum halides tested, $LaBr_3$ provided remarkable enantioselectivity (83% ee), but the enantioselectivity was dependent on catalyst loading and less reproducible, possibly due to its poor solubility (entries 3,4). The use of La(OTf)$_3$ as a soluble lanthanum salt hardly improved the enantioselectivity (entry 6). Based on the fact that nitrate anions enhance the solubility of lanthanide complex,[20] $^n$Bu$_4$N(NO$_3$) was added to the reaction using $LaCl_3$, which significantly improved the enantioselectivity to 82% ee (entry 1 vs entry 7). $NH_4NO_3$ was also effective for catalytic efficiency (entry 8). Eventually, La(NO$_3$)$_3$•6H$_2$O was identified as the best lanthanum source for our purpose due to its relatively high solubility in AcOEt, stability to moisture, commercial availability in large quantities, and low cost ($443/500 g, Aldrich),[19] affording the amination product in 95% yield and 68% ee and the catalyst loading can be reduced to 2.5 mol % (entries 9,10).[21]

Because additional base can promote the background reaction leading to racemic product and/or be directly involved in the transition state, the character of the base was expected to have a significant impact on enantioselectivity. Thus, we next examined other bases in combination with La(NO$_3$)$_3$•6H$_2$O (Table 2). We anticipated that amine bases located in near proximity to $La^{3+}$ by coordination and worked cooperatively with La(NO$_3$)$_3$•6H$_2$O and ligand (*R*)-**3a**,[22] preventing the undesirable background reaction promoted by the base itself. Indeed, generally higher enantioselectivity was observed in the reaction using various amine bases. Of particular note is that the structure of the amines, including their stereochemistry, was a determining factor for enantioselectivity in the reaction,

(18) For an alternative enantioselective synthetic approach toward AS-3201, see: Watanabe, T.; Kawabata, T. *Heterocycles* **2008**, *76*, 1593.
(19) *Sigma-Aldrich Handbook of Fine Chemicals 2009−2010*; Sigma-Aldrich: Milwaukee, WI, 2008.
(20) (a) Hayano, T.; Sakaguchi, T.; Furuno, H.; Ohba, M.; Okawa, H.; Inanaga, J. *Chem. Lett.* **2003**, *32*, 608. (b) Furuno, H.; Hayano, T.; Kambara, T.; Sugimoto, Y.; Hanamoto, T.; Tanaka, Y.; Jin, Y. Z.; Kagawa, T.; Inanaga, J. *Tetrahedron* **2003**, *59*, 10509.
(21) Recent examples for the use of lanthanide nitrates for asymmetric catalysis, see: (a) Hamada, T.; Manabe, K.; Ishikawa, S.; Nagayama, S.; Shiro, M.; Kobayashi, S. *J. Am. Chem. Soc.* **2003**, *125*, 2989, and ref 20b. Lanthanide nitrates generally exhibit much less catalytic efficiency compared with corresponding triflates. For example, see: (b) Kano, S.; Nakano, H.; Kojima, M.; Baba, N.; Nakajima, K. *Inorg. Chim. Acta* **2003**, *349*, 6.

***Table 2.*** Catalytic Asymmetric Amination of **1** with $La(NO_3)_3$/(*R*)-**3a**/base Ternary Catalyst[a]

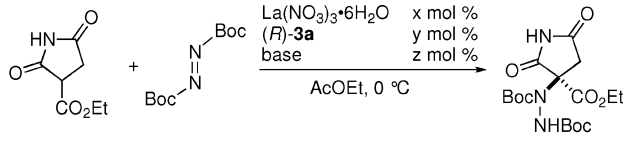


| entry | *x* | *y* | base | *z* | time | yield[b] (%) | ee (%) |
|---|---|---|---|---|---|---|---|
| 1 | 2.5 | 5 | − | − | 18 h | 71 | 0 |
| 2 | 2.5 | 5 | KO$^t$Bu | 7.5 | 180 min | >99 | 58 |
| 3 | 2.5 | 5 | $Et_3N$ | 7.5 | 120 min | >99 | 79 |
| 4 | 2.5 | 5 | $Et_2NH$ | 7.5 | 120 min | >99 | 52 |
| 5 | 2.5 | 5 | $^t$BuNH$_2$ | 7.5 | 60 min | >99 | 70 |
| 6 | 2.5 | 5 | 2,6-lutidine | 7.5 | 330 min | >99 | 35 |
| 7 | 2.5 | 5 | H-D-Phe-O$^t$Bu | 7.5 | 20 min | >99 | 89 |
| 8 | 2.5 | 5 | H-D-Val-O$^t$Bu | 7.5 | 20 min | >99 | 91 |
| 9 | 2.5 | 5 | H-L-Val-O$^t$Bu | 7.5 | 90 min | >99 | 80 |
| 10 | 2.5 | 2.5 | H-D-Val-O$^t$Bu | 7.5 | 20 min | >99 | 91 |
| 11 | 2.5 | 0 | H-D-Val-O$^t$Bu | 7.5 | 120 min | >99 | −1 |
| 12 | 0 | 5 | H-D-Val-O$^t$Bu | 7.5 | 24 h | 92 | 13 |
| 13 | 0.5 | 0.5 | H-D-Val-O$^t$Bu | 1.5 | 1 h | >99 | 90 |

[a] **1**: 0.4 mmol, BocN=NBoc: 0.48 mmol. [b] Determined by $^1$H NMR analysis with $Bn_2O$ as an internal standard.

implying that the amines are involved in the transition state. The reaction with simple achiral amine bases (1°, 2°, 3° alkylamines, 2,6-lutidine) completed using 2.5 mol % of catalyst, but the enantioselectivity remained unsatisfactory (entries 3−6). Assuming that 2 molecules of (*R*)-**3a** to $La^{3+}$ are needed to construct a favorable transition state in the first-generation catalyst using $La(O^iPr)_3$, amines with the substructure of ligand (*R*)-**3a** were examined. As shown in entries 7−9, the reaction with α-amino acid $^t$Bu esters as additional amines significantly improved the enantioselectivity. In particular, H-D-Val-O$^t$Bu exhibited the best performance in terms of both catalytic activity and enantioselectivity (entry 8, 91% ee).[23] Intriguingly, the use of an antipode, H-L-Val-O$^t$Bu, resulted in inferior enantioselectivity compared with H-D-Val-O$^t$Bu (entry 9), indicating that additional amines are at work under an asymmetric environment. In this La/(*R*)-**3a**/amine ternary catalyst system, the ratio of La/(*R*)-**3a** was reduced to 1:1 without any detrimental effect (entries 8 vs10). The attempted reaction in the absence of either (*R*)-**3a** or $La(NO_3)_3$•$6H_2O$ gave nearly racemic product **6**, (entries 11,12), verifying the significance of the ternary catalyst system of (*R*)-**3**/$La(NO_3)_3$•$6H_2O$/amine to exert high catalytic efficiency. The catalyst loading can be reduced to as little as 0.5 mol % and the reaction at 0 °C maintained high enantioselectivity (entry 13). The second-generation catalytic asymmetric amination was successfully performed on a 100-g scale with 1 mol % of catalyst prepared from $La(NO_3)_3$•$xH_2O$,[24] affording the desired product in 96% yield (2 steps) and 91% ee after removal of Boc groups under acidic conditions (Scheme 4).[14b]

***Scheme 4.*** One-Hundred Gram Scale Demonstration of the Second-Generation Catalytic Asymmetric Amination

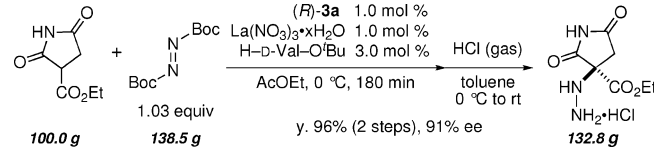


**Catalytic Asymmetric Amination of *N*-Nonsubstituted α-Alkoxycarbonyl Amides.** Optically active *N*-nonsubstituted α-amino-α-alkoxycarbonyl amides constitute useful chiral building blocks for the synthesis of biologically active compounds. Several heterocycles have been synthesized from this class of compounds.[25] Catalytic asymmetric amination of *N*-nonsubstituted α-alkoxycarbonyl amides **7** allows for efficient access to this class of compounds in an enantiomerically enriched form, however, to the best of our knowledge, there are no catalytic asymmetric transformations utilizing *N*-nonsubstituted α-alkoxycarbonyl amides **7** as substrates.[26,27] The expected difficulties with a catalytic asymmetric reaction of **7** are: (1) a relatively high p*K*a of the α-C−H proton compared with other representative active methylene compounds;[28] (2) competitive deprotonation of the α-C−H proton and kinetically more labile amide N−H protons;[29] and (3) a multiple coordination pattern of **7** leading to poor enantioselectivity. In this context, we anticipated that the lanthanum/amide-based ligand catalytic system described above would be suitable for these substrates, in which coordination to La and hydrogen bonding would cooperatively activate the substrates and control the stereochemical course of the reaction. Indeed, the succinimide derivative **1** contains the substructure of α-alkoxycarbonyl amide **7**, and the substandard enantioselectivity observed in the reaction with *N*-Me protected derivative **8** suggested that the catalyst would recognize the nonprotected α-alkoxycarbonyl amide **7** including the *trans*-amide N−H proton as a privileged structure (Scheme 5). Therefore, we applied the second-generation ternary catalytic system to the catalytic asymmetric amination of **7**. Initially, α-phenyl-α-ethoxycarbonyl amide **7a** was selected as a representative substrate and subjected to the second-generation amination conditions with di-*tert*-butyl azodicarboxylate (Scheme 6). Using 10 mol % of catalyst, the desired amination product

(22) Selected examples of rare earth metal asymmetric catalyst showing enhanced stereoselectivity in the presence of amine, see: (a) Kobayashi, S.; Ishitani, H. *J. Am. Chem. Soc.* **1994**, *116*, 4083. (b) Kobayashi, S.; Ishitani, H.; Hachiya, I.; Araki, M. *Tetrahedron* **1994**, *50*, 11623. (c) Kobayashi, S.; Kawamura, M. *J. Am. Chem. Soc.* **1998**, *120*, 5840. (d) Furuno, H.; Hanamoto, T.; Sugimoto, Y.; Inanaga, J. *Org. Lett.* **2000**, *2*, 49. (e) Fukuzawa, S.-I.; Komuro, Y.; Nakanao, N.; Obata, S. *Tetrahedron Lett.* **2003**, *44*, 3671. See also ref 16a.

(23) When $LaBr_3$ was used instead of $La(NO_3)_3$•$6H_2O$, the product (−)-**6** was obtained in 97% yield and 72% ee after 13 h at 0 °C.

(24) $La(NO_3)_3$•$xH_2O$ (99.9% purity, $186.5/500 g, Aldrich (ref 19)) is less expensive than $La(NO_3)_3$•$6H_2O$.

(25) (a) Hermann, P.; Eduard, E.; Hans-Dietrich, S.; Andreas, W.; Kurt, P. *J. Heterocyclic Chem.* **2000**, *37*, 839. (b) Lyubomir, R. D.; Wolfgang, F.; Ivanov, I. C. *Synlett* **2004**, 1584. (c) Li, S.; Wang, S. *J. Heterocyclic Chem.* **2008**, *45*, 1875. (d) Bambang, P.; Robert, S. K.; Thomas, P. C. *Synlett* **1992**, 231.

(26) For catalytic asymmetric fluorination of *N*-unsubstituted α-*tert*-butoxycarbonyl *lactams*, see: (a) Suzuki, T.; Oto, T.; Hamashima, Y.; Sodeoka, M. *J. Org. Chem.* **2007**, *72*, 246. For a partially successful 1,4-reduction of unsaturated primary amide and the following enantioselective protonation by asymmetric catalysts (1 example, 50% ee), see: (b) Ohtsuka, Y.; Ikeno, T.; Yamada, T. *Tetrahedron: Asymmetry* **2003**, *14*, 967. For a review of enzymatic kinetic resolution of primary amides, see: (c) Wang, M.-X *Top. Catal.* **2005**, *35*, 117, and references cited therein.

(27) Diastereoselective reactions using *N*-nonsubstituted α-alkoxycarbonyl amides as substrates, see: Kozlowski, M. C.; DiVirgilio, E. S.; Malolanarasimhan, K.; Mulrooney, C. A. *Tetrahedron: Asymmetry* **2005**, *16*, 3599. Catalytic transformation utilizing *N*-nonsubstituted α-alkoxycarbonyl amides, see: Zhang, J.; Sarma, K. D.; Curran, T. T.; Belmont, D. T.; Davidson, J. G. *J. Org. Chem.* **2005**, *70*, 5890.

(28) p*K*a of α-C-H proton of **7a** is 21.3, which was calculated at the B3LYP/6-31G+(d,p) level. For details, see Supporting Information.

(29) p*K*a of *cis*- and *trans*-amide N−H protons of **7a** is 24.0, and 27.8, respectively, which was calculated at the B3LYP/6-31G+(d,p) level. For details, see supporting information. Whereas N−H protons are less acidic thermodynamically, they are expected to be kinetically more labile, compromising effective deprotonation of α-C−H proton.

***Scheme 5.*** Expected Privileged Structure for Catalytic Asymmetric Amination with $La(NO_3)_3$/(*R*)-**3a**/base Ternary Catalyst

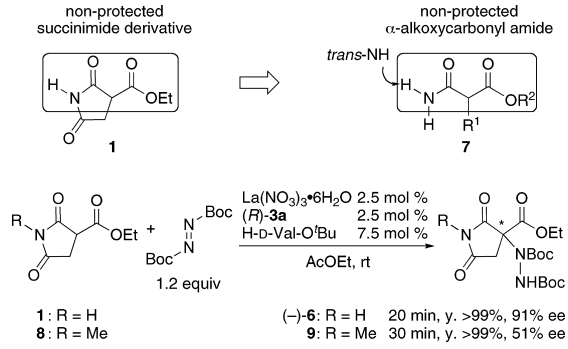


***Scheme 6.*** Catalytic Asymmetric Amination of Nonprotected α-Ethoxycarbonyl Amide **7a** and Its *N*-Alkylated Derivatives **10**,**11**

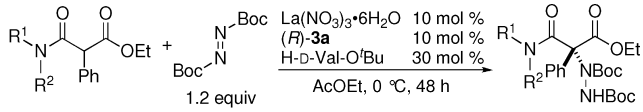


**7a**: $R^1 = R^2 = H$ — **12a**: $R^1 = R^2 = H$ y. 83%, 99% ee
**10**: $R^1$ = Me, $R^2 = H$ — **13**: $R^1$ = Me, $R^2 = H$ y. ND
**11**: $R^1 = R^2$ = Me — **14**: $R^1 = R^2$ = Me y. ND

***Table 3.*** Catalytic Asymmetric Amination of Nonprotected α-Alkoxycarbonyl Amides **7** with the Second-Generation Catalyst[a]

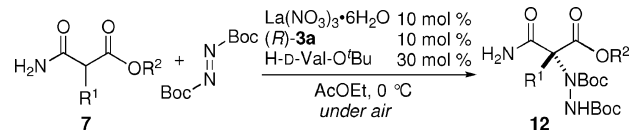


| | α-alkoxycarbonyl amide **7** | | | | | | |
|---|---|---|---|---|---|---|---|
| entry | $R^1$ | $R^2$ | | product | time (h) | yield[b] (%) | ee (%) |
| 1 | Ph | Et | **7a** | **12a** | 48 | 83 | >99 |
| 2 | Ph | Me | **7b** | **12b** | 24 | 92 | >99 |
| 3 | 4-$FC_6H_4$ | Me | **7c** | **12c** | 14 | 99 | >99 |
| 4 | 2-$FC_6H_4$ | Et | **7d** | **12d** | 48 | 45 | 94 |
| 5 | 4-$CF_3C_6H_4$ | Me | **7e** | **12e** | 14 | 94 | >99 |
| 6 | 4-$NO_2C_6H_4$ | Et | **7f** | **12f** | 10 | >99 | 99 |
| 7 | 4-$MeOC_6H_4$ | Et | **7g** | **12g** | 48 | 88 | 99 |
| 8 | 4-$MeC_6H_4$ | Et | **7h** | **12h** | 12 | 92 | 99 |
| 9 | 2-naphthyl | Et | **7i** | **12i** | 18 | >99 | >99 |
| 10 | 3-thienyl | Et | **7j** | **12j** | 15 | >99 | >99 |
| 11 | 3-pyridyl | Et | **7k** | **12k** | 12 | 70 | >99 |
| 12 | Me | Et | **7l** | **12l** | 45 | 98 | 83 |

[a] **7**: 0.2 mmol, BocN ═NBoc: 0.24 mmol. [b] Isolated yield.

**12a** bearing a tetrasubstituted stereogenic carbon was obtained with nearly perfect enantioselectivity, although the reaction was sluggish, likely due to the higher p*K*a of the α-C−H proton than that of **1**. In contrast to **7a**, the amination reaction hardly proceeded with *trans*-*N*-Me **10** or the *N*,*N*-dimethyl derivative **11**, indicating that hydrogen bonding through *trans*-N−H of **7a** was crucial for the recognition/activation of substrates (Scheme 5). The substrate scope of the catalytic asymmetric amination of **7** is summarized in Table 3. Methyl ester analog **7b** exhibited higher reactivity to afford **12b** in 99% yield and >99% ee after 24 h (entry 2). Generally excellent enantioselectivity was observed and the electronic properties of the aromatic ring at the α-position were responsible for the reaction rate. Substrates bearing an electron-withdrawing group resulted in a rapid reaction (entries 3,5,6), whereas the reaction proceeded sluggishly with **7g**, which has an electron-donating methoxy group (entry 7). **7d** showed unexpectedly low reactivity, probably because **7d** was reluctant to form a planar enolate due to steric or electrostatic repulsion of 2-fluoro substituent (entry 4). Notably, even a substrate with a strongly coordinative pyridyl group exhibited high enantioselectivity (entry 11). This would be attributed to the preferential coordination of **7k** to the catalyst through the privileged substructure shown in Scheme 5. The enantioselectivity of the asymmetric amination of α-alkyl substrates **7l** was not as high as that of aromatic and heteroaromatic substrates, providing the product **12l** in 98% yield and 83% ee (entry 14). The obtained amination product (+)-**12a** was successfully converted to a hydantoin derivative (−)-**16** (Scheme 7).[30] The compound (+)-**12a** (>96% ee) was treated with concentrated hydrochloric acid to remove the Boc group, followed by N−N bond cleavage by Raney nickel to afford the α, α-disubstituted α-amino acid derivative (+)-**15** in 98% yield in 2 steps. Subsequent reaction with *p*-nitophenyl chloroformate buffered with $NaHCO_3$ afforded hydantoin derivative (−)-**16** in 83% yield,[31] the absolute configuration of which was determined by X-ray crystallographic analysis.[32] The present protocol provides an efficient new entry to access enantioenriched α,α-disubstituted amino acid derivatives and hydantoins bearing a stereogenic tetrasubstituted carbon, which are important structural motifs in medicinal chemistry.[33]

***Scheme 7.*** Transformation of the Amination Product (+)-**12** to Hydantoin (−)-**16**[a]

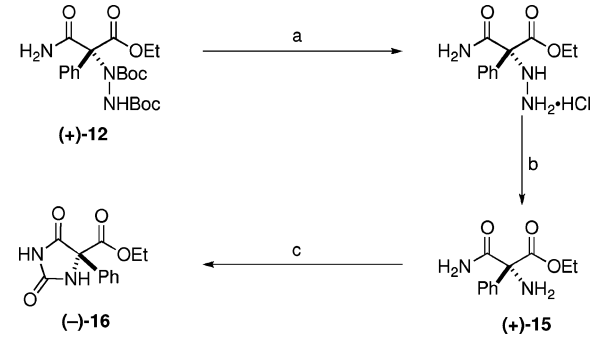


[a] Reagents and conditions: (a) HCl (g), toluene, 0 °C, 1 h, 98%; (b) Raney-Ni, $H_2$, EtOH/AcOH = 3/2, rt, 3 h, >99%; (c) (i) *p*-nitrophenyl chloroformate, $CH_3CN$, $NaHCO_3$, rt, 1 h; (ii) $H_2O$, rt, 1.5 h, 83%.

**Mechanistic Studies of the $La(NO_3)_3$/(R)-3a/H-D-Val-O$^t$Bu Ternary Amination Catalyst.** The utility of the $La(NO_3)_3$/(*R*)-**3a**/H-D-Val-O$^t$Bu ternary catalytic system for highly coordinative substrates led us to examine the mechanistic details. ESI MS spectra of the first-generation catalyst ($La(O^iPr)_3$/**3a** = 1/2

(30) For the rich chemistry and property of hydantoins, see: (a) Ware, E. *Chem. Rev.* **1950**, *46*, 403. For a leading examples of the racemic synthesis of hydantoins, see: (b) Rizzi, J. P.; Schnur, R. C.; Hutson, N. J.; Kraus, K. G.; Kelbaugh, P. R. *J. Med. Chem.* **1989**, *32*, 1208. (c) Kim, D.; et al. *Bioorg. Med. Chem. Lett.* **2001**, *11*, 3099. (d) Sheppeck, J. E.; Gilmore, J. L.; Tebben, A.; Xue, C.-B.; Liu, R.-Q.; Decicco, C. P.; Duan, J. J.-W. *Bioorg. Med. Chem. Lett.* **2007**, *17*, 2769. (e) Zhao, B.; Du, H.; Shi, Y. *J. Am. Chem. Soc.* **2008**, *130*, 7220.

(31) Yamaguchi, J.; Harada, M.; Kondo, T.; Noda, T.; Suyama, T. *Chem. Lett.* **2003**, *32*, 372.

(32) For details, see Supporting Information.

(33) (a) Comber, R. N.; Reynolds, R. C.; Friedrich, J. D.; Manguikian, R. A.; Buckheit, R. D. Jr.; Truss, J. W.; Shannon, W. M.; Secrist, J. A. *J. Med. Chem.* **1992**, *35*, 3567. (b) Brouillette, W. J.; Jestkov, V. P.; Brown, M. L.; Akhtar, M. S.; DeLorey, T. M.; Brown, G. B. *J. Med. Chem.* **1994**, *37*, 3289. (c) Stilz, H. U.; Guba, W.; Jablonka, B.; Just, M.; Klingler, O.; König, W.; Wehner, V.; Zoller, G. *J. Med. Chem.* **2001**, *44*, 1158. (d) Muccioli, G. G.; Fazio, N.; Scriba, G. K. E.; Poppitz, W.; Cannata, F.; Poupaert, J. H.; Wouters, J.; Lambert, D. M. *J. Med. Chem.* **2006**, *49*, 417.

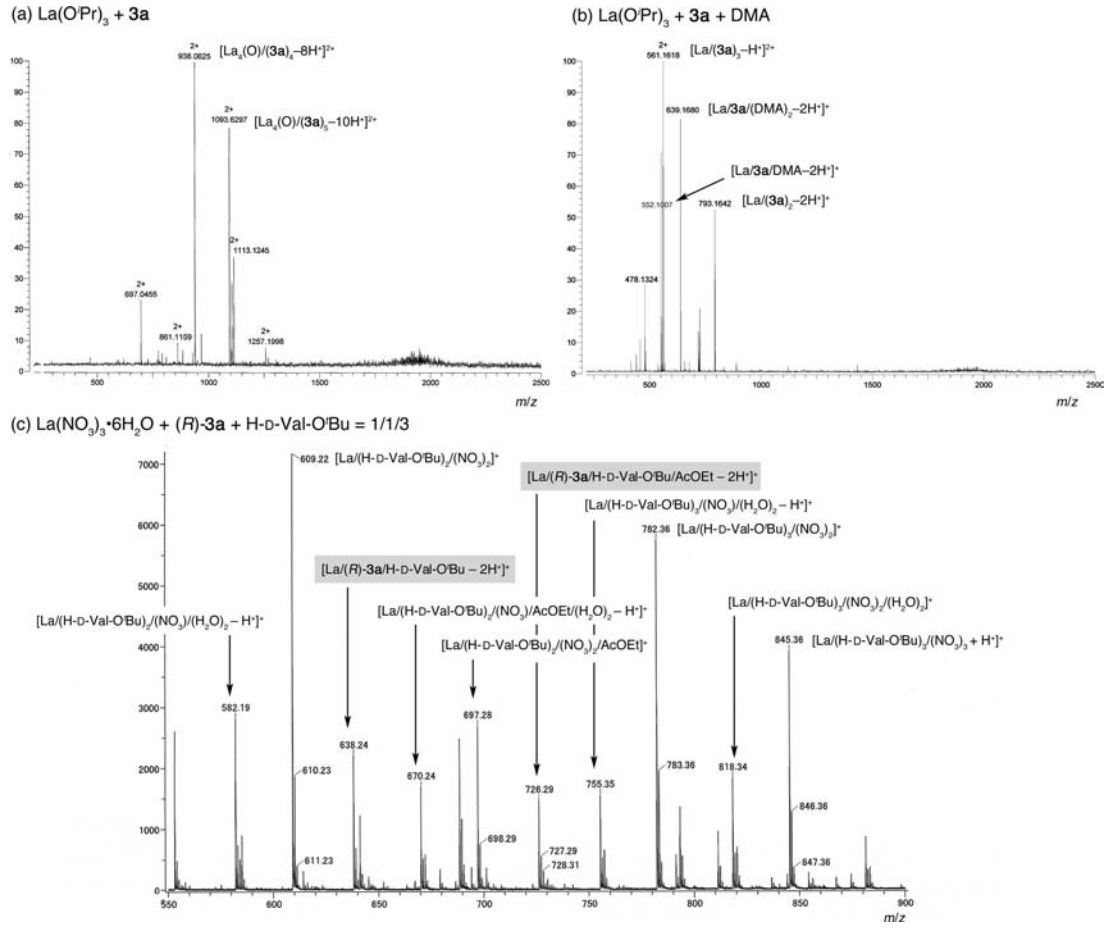


***Figure 1.*** ESI MS analysis of La catalyst solution in positive ion mode. (a) La(O$^i$Pr)$_3$/**3a** = 1/2; (b) La(O$^i$Pr)$_3$/**3a** = 1/2 with DMA (*N*,*N*-dimethylacetamide); (c) La(NO$_3$)$_3$•6H$_2$O/(*R*)-**3a**/H-D-Val-O$^t$Bu = 1/1/3.

with or without DMA) and the second-generation catalyst (La(NO$_3$)$_3$/(*R*)-**3a**/H-D-Val-O$^t$Bu = 1/1/3) are shown in Figure 1. In contrast to the oligomeric La/**3a** complexes observed in the MS spectrum of the first-generation catalyst in the absence of DMA (Figure 1a), a peak derived from monomeric lanthanum species became dominant by the addition of DMA to the catalyst solution (Figure 1b). Based on the higher catalytic efficiency and reproducibility in the presence of DMA,[14a] we assume that the monometallic lanthanum species was involved in the desired enantioselective pathway. This assumption was further supported by the MS analysis of the second-generation catalyst, which displayed generally higher catalytic activity and reproducibility compared to the first-generation catalyst. In the MS spectrum of the second-generation catalyst solution prepared from La(NO$_3$)$_3$/(*R*)-**3a**/H-D-Val-O$^t$Bu = 1/1/3 (Figure 1c), only monometallic lanthanum complexes appeared, probably because highly coordinative and bidentate nitrate anions circumvented the formation of unfavorable multimetallic aggregates. Together with partially associated La complexes, the peaks derived from a ternary complex of [La(NO$_3$)$_3$/(*R*)-**3a**/H-D-Val-O$^t$Bu]$^+$ ($m/z$ = 638) and [La(NO$_3$)$_3$/(*R*)-**3a**/H-D-Val-O$^t$Bu/AcOEt]$^+$ ($m/z$ = 726) appeared, supporting the notion that the additional amine base H-D-Val-O$^t$Bu coordinates to lanthanum and is involved in the transition state.[34] This observation is consistent with the fact that the enantioselectivity of the amination was dependent on the three-dimensional structure of the additional amine bases (Table 2). In the MS analysis of the first-generation catalyst with DMA and the second-generation catalyst, we observed no peaks derived from a multimetallic lanthanum complex. Preventing undesired lanthanum aggregation would be key to the high catalyst turnover and high reproducibility.

To gain further insight into the actual active species, we conducted several $^1$H NMR experiments. The $^1$H NMR spectrum of La(NO$_3$)$_3$/(*R*)-**3a** = 1:1 in THF-$d_8$ was essentially identical to that of (*R*)-**3a** itself, indicating that no appreciable association occurred between neutral La(NO$_3$)$_3$ and (*R*)-**3a** in the absence of a base.[35] Indeed, any attempts of crystallization from La(NO$_3$)$_3$/(*R*)-**3a** = 1:1 in AcOEt resulted in the recovery of the crystal of La(NO$_3$)$_3$•$x$H$_2$O. In the presence of H-D-Val-O$^t$Bu (3 equivalents to La), substantial peak broadening was observed in $^1$H NMR spectrum of the ternary catalyst solution, indicating that complexation occurred in the presence of additional base and that the assembly of La$^{3+}$, (*R*)-**3a**, and H-D-Val-O$^t$Bu were in equilibrium within NMR time scale.[32] The negligible change in the CD spectrum of the ternary catalyst solution from that of (*R*)-**3a** itself suggested that any possible complexation was in equilibrium and the dissociated state was dominant.[32] Any

(34) The peaks derived from the ternary complex were observed even in the presence of substrate **7c**. See Supporting Information.

(35) Only the peaks derived from [(*R*)-**3a** + H$^+$]$^+$ and [((*R*)-**3a**)$_2$ + H$^+$]$^+$ appeared predominantly in ESI MS spectrum of La(NO$_3$)$_3$/(*R*)-**3a** = 1:1 solution. Catalytic asymmetric amination of **7a** proceeded in THF solvent to give the product **12a** in comparable yield and enantioselectivity (10 mol % of catalyst, 0 °C, 45 h, 91% yield, 96% ee). For details of NMR and ESI MS analysis, see Supporting Information.

***Table 4.*** Reexamination of Base Effect in the Second-generation Catalytic Asymmetric Amination of **7c**[a]

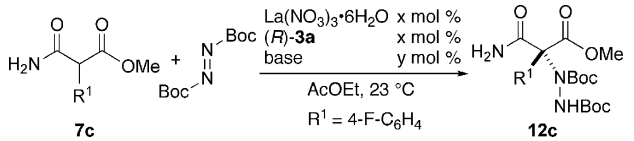


| | | base (y mol %) | | | | | | | |
|---|---|---|---|---|---|---|---|---|---|
| entry | *x* | H-D-Val-O$^t$Bu | $Et_3N$ | $Cs_2CO_3$ | $v_{obs}$ (mM min$^{-1}$) | key[b] | time (h) | yield[c] (%) | ee (%) |
| 1 | 4 | 12 | – | – | 1.16 | ● | 10 | 85 | 96 |
| 2 | 4 | – | 12 | – | 0.24 | ■ | 10 | 75 | 90 |
| 3 | 4 | – | – | 12 | 0.10 | ▲ | 10 | 53 | 88 |
| 4 | 4 | 4 | 8 | – | 1.35 | □ | 10 | >99 | 98 |
| 5 | 4 | 4 | – | 8 | 1.27 | ○ | 10 | >99 | 98 |

[a] **7c**: 0.4 mmol, BocN=NBoc: 0.48 mmol. [b] Key in Figure 2. [c] Determined by $^1$H NMR with $Bn_2O$ as an internal standard.

attempts to crystallize the second-generation catalyst mixture La(NO$_3$)$_3$/(*R*)-**3a**/H-D-Val-O$^t$Bu = 1:1:3 gave rise to the exclusive crystallization of the H-D-Val-O$^t$Bu•$HNO_3$ salt.[36]

On the basis of the NMR and ESI MS analyses, the additional amine base would deprotonate the phenolic proton of (*R*)-**3a**, facilitating the complexation of La(NO$_3$)$_3$ and (*R*)-**3a** in equilibrium. The correlation of the observed enantioselectivity of the amination and the three-dimensional structure of the amine bases (Table 2) clearly indicated that the function of additional base is not only deprotonation, but also the enhancement of enantioselection through participation in the transition state. Although the catalyst components were in equilibrium between the associated and dissociated states, a La(NO$_3$)$_3$/(*R*)-**3a**/H-D-Val-O$^t$Bu ternary complex, which was indeed observed in MS analysis in Figure 1c, was anticipated to be catalytically much more active than the dissociated or partially complexed state. To examine this assumption, a kinetic profile of the asymmetric amination of α-alkoxycarbonyl amides **7c** with amine bases (H-D-Val-O$^t$Bu or $Et_3N$), inorganic base ($Cs_2CO_3$), and mixed-base (H-D-Val-O$^t$Bu/$Et_3N$ or H-D-Val-O$^t$Bu/$Cs_2CO_3$) conditions was developed (Table 4, Figure 2).[37] The initial rate of the reaction with H-D-Val-O$^t$Bu ($v$ = 1.16 mM min$^{-1}$, solid circles) was substantially faster than that with $Et_3N$ ($v$ = 0.24 mM min$^{-1}$, solid triangles) or $Cs_2CO_3$ ($v$ = 0.10 mM min$^{-1}$, solid squares). Moreover, the enantioselectivity in the reaction with H-D-Val-O$^t$Bu was higher than that with $Et_3N$ or $Cs_2CO_3$ (Table 4, entries 1−3, Figure 2). This would be due to the fact that amine bases coordinated to the La/(*R*)-**3a** complex to form the ternary complex in equilibrium, which recognized/activated the substrates by harnessing a cooperative noncovalent interaction of coordination to $La^{3+}$ and hydrogen bonding, leading to a higher reaction rate and enantioselectivity. The advantage of H-D-Val-O$^t$Bu over $Et_3N$ for the reaction rate would be ascribed to smaller steric factor and possible bidentate coordination through an ester carbonyl group, facilitating the coordination of H-D-Val-O$^t$Bu to $La^{3+}$ to form the ternary catalyst in equilibrium, a tentative actual active catalyst. The coordinated H-D-Val-O$^t$Bu reinforced the enantioselection as an additional chiral entity of the ternary catalyst. Remarkably, the reaction rate and enantioselectivity recovered with mixed-base conditions (H-D-Val-O$^t$Bu/$Et_3N$, H-D-Val-O$^t$Bu/$Cs_2CO_3$), exhibiting a comparable reaction profile and enantioselectivity as that obtained under the standard conditions using H-D-Val-O$^t$Bu as the sole base (Table 4, entries 1 vs 4, 1 vs 5, Figure 2, open squares and open circles). This observation further supported the above assumption and implied a dual role of H-D-Val-O$^t$Bu; (1) the deprotonation of (*R*)-**3a** to facilitate the association of $La^{3+}$ and (*R*)-**3a**; and (2) the coordination to $La^{3+}$ as an additional ligand working cooperatively with $La^{3+}$ to recognize/activate substrates (Scheme 8a).[38] In the mixed-base system, $Et_3N$ or $Cs_2CO_3$ worked solely to deprotonate (*R*)-**3a** to shift the equilibrium to form a greater fraction of the La/(*R*)-**3a** complex than that formed in the standard conditions (La(NO$_3$)$_3$/(*R*)-**3a**/H-D-Val-O$^t$Bu = 1/1/3);[39] subsequently H-D-Val-O$^t$Bu coordinated to La/(*R*)-**3a** to form a ternary complex, enhancing the reaction rate and enantioselection (Scheme 8b).[40] Taking advantage of the preferential coordination of H-D-Val-O$^t$Bu, the catalyst loading was successfully reduced to as little as 0.5 mol % with the aid of additional base (Table 5). This mixed-base catalytic system highlighted the fact that neither $Et_3N$ nor the La/(*R*)-**3a** complex worked as an efficient catalyst and the ternary catalyst including H-D-Val-O$^t$Bu was involved in the highly enantioselective reaction pathway. $Et_3N$ worked solely to deprotonate (*R*)-**3a**, thereby increasing the molar fraction of La/(*R*)-**3a**, leading to a greater molar fraction of the ternary complex in combination with H-D-Val-O$^t$Bu.[40] The mixed-base conditions were applicable to several α-alkoxycarbonyl amides **7**, affording product **12** in excellent yield and comparable enantioselectivity with 0.5−3 mol % of catalyst loading.[41]

The asymmetric amination was then performed with partially resolved ligand (*R*)-**3a**. $NEt_3$ was used as an additional base instead of H-D-Val-O$^t$Bu because the combination of (*S*)-**3a** and H-D-Val-O$^t$Bu is a mismatched pair (Table 1, entry 9) and the interpretation of the data was complicated. The reactions were conducted with 2.5 mol % of the second-generation catalyst and completed after 90 min of stirring at room temperature. As

(36) The H-D-ValO$^t$Bu deprotonated (*R*)-**3a** to form H-D-Val-O$^t$Bu•$HNO_3$ salt. Although the deprotonation/protonation would be in equilibrium, H-D-Val-O$^t$Bu•$HNO_3$ was highly crystalline and preferencially crystallized.

(37) A kinetic study using substrate **1** provided unreliable data due to a background reaction under basic or acidic conditions at the work-up stage. The data on the kinetic study of **7c** is detailed in the Supporting Information.

(38) As La/H-D-Val-O$^t$Bu complex was observed in ESI MS (Figure 1c), an alternative pathway to form the ternary complex through the coordination of H-D-Val-O$^t$Bu to $La^{3+}$ to give La/H-D-Val-O$^t$Bu and subsequent coordination of (*R*)-**3a** is also feasible. The catalytic asymmetric amination reaction of **7c** in the absence of (*R*)-**3a** was very sluggish (room temperature, 25 h, 18% yield) and the enantioselectivity of the product was poor (4% ee), indicating that La/H-D-Val-O$^t$Bu was as poor a catalyst as La/(*R*)-**3a**.

(39) The mixed-base conditions exhibited higher reaction rate as shown in Table 4, entries 1, 4, and 5. This observation is likely explained by assuming that H-D-Val-O$^t$Bu was less effective for the deprotonation of (*R*)-**3a** due to extensive coordination to $La^{3+}$ as shown in ESI MS spectrum of La(NO$_3$)$_3$/(*R*)-**3a**/H-D-Val-O$^t$Bu = 1/1/3 (Figure 1c).

(40) In ESI MS spectrum of the mixed-base catalyst solution (La/(*R*)-**3a**/H-D-Val-O$^t$Bu/$Et_3N$ = 1/1/1/2), the peaks derived from the ternary complexes including La, (*R*)-**3a**, and H-D-Val-O$^t$Bu were observed, whereas no peaks derived from the complexes containing $Et_3N$ were identified. See Supporting Information for details.

(41) In the standard reaction conditions using H-D-Val-O$^t$Bu as the sole base, 3 mol equiv of H-D-Val-O$^t$Bu was required for high catalytic efficiency and enantioselectivity, likely because 2 mol equiv of H-D-Val-O$^t$Bu was consumed for the deprotonation of (*R*)-**3a** (although protonation/deprotonation was in equilibrium) and the apparent amount of H-D-Val-O$^t$Bu was 1 mol equiv to La(NO$_3$)$_3$. In the mixed-base conditions, 3 mol equiv of $Et_3N$ was expected to deprotonate (*R*)-**3a**, thereby 1 mol equiv of H-D-Val-O$^t$Bu appeared to be sufficient. Three mol equiv of H-D-Val-O$^t$Bu, however, were still required to assure the high catalytic efficiency and enantioselectivity. Thus, 3 mol equiv of H-D-Val-O$^t$Bu to La(NO$_3$)$_3$ were employed to form the ternary complex irrespective of its protonation.

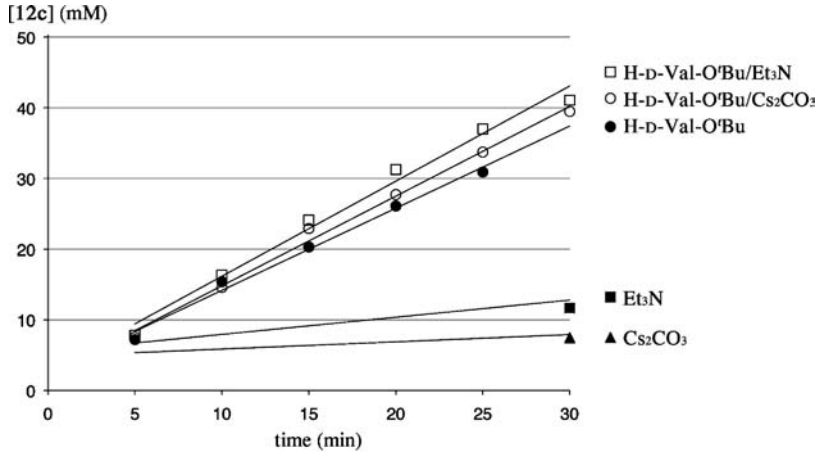


***Figure 2.*** Kinetic profiles of the asymmetric amination of **7c** promoted by $La(NO_3)_3$•$6H_2O$/(*R*)-**3a**/base = 1/1/3 catalyst. The reactions were run with [**7c**] = 100 mM, [BocN=NBoc] = 120 mM, [$La(NO_3)_3$•$6H_2O$] = 2.5 mM, [(*R*)-**3a**] = 2.5 mM, and [base] = 7.5 mM (4 mol % of catalyst loading based on La). ●: base = H-D-Val-O'Bu (corresponds to Table 4, entry 1), ■: base = $Et_3N$ (entry 2), ▲: base = $Cs_2CO_3$ (entry 3), □: base = H-D-Val-O'Bu/$Et_3N$ (1/2) (entry 4), ○: base = H-D-Val-O'Bu/$Cs_2CO_3$ (1/2) (entry 5).

***Scheme 8.*** Proposed Dual Role of Additional Amine Base in the Second-Generation Amination Reaction

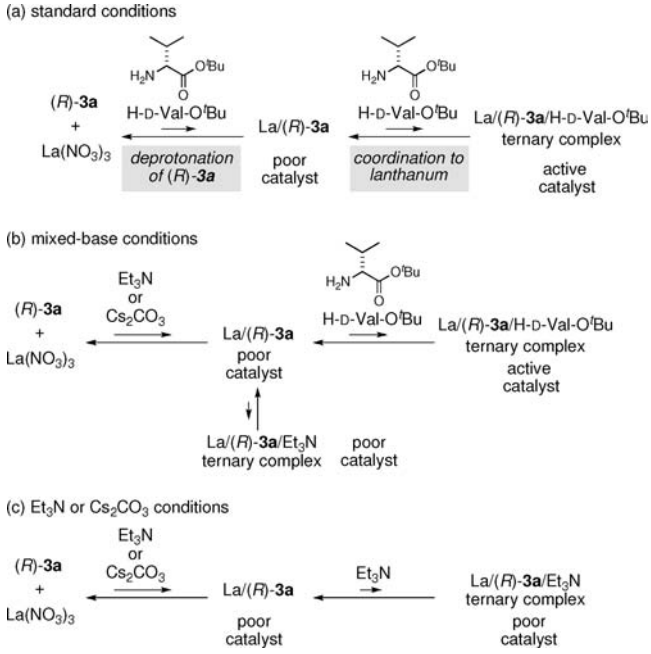


shown in Figure 3, a linear relationship was observed between the enantiopurity of (*R*)-**3a** and the enantioselectivity of (−)-**6**.[42] Subsequent kinetic studies of the second-generation catalyst using **7c** as the substrate indicated that the reaction was dependent on the initial concentration of the catalyst components. From these observations, the most likely scenario is that the coordination of (*R*)-**3a** to $La^{3+}$ was induced by a base and the association was in equilibrium. The coordination of H-D-Val-O'Bu to the monomeric La/(*R*)-**3a** complex furnished the ternary complex, which allowed the enantioselective pathway to proceed, likely through the monomeric lanthanum complex furnished with (*R*)-**3a** and H-D-Val-O'Bu.[38]

Because the catalyst components were in equilibrium between the associated and dissociated states, the structural and functional

(42) Girard, C.; Kagan, H. B. *Angew Chem., Int. Ed.* **1998**, *37*, 2922. (b) Blackmond, D. G. *Acc. Chem. Res.* **2000**, *33*, 402. (c) Satyanarayana, T.; Abraham, S.; Kagan, H. B. *Angew. Chem., Int. Ed.* **2009**, *48*, 456.

***Table 5.*** Second-Generation Catalytic Asymmetric Amination of **7** with H-D-Val-O'Bu/$Et_3N$ Mixed-Base System[a]

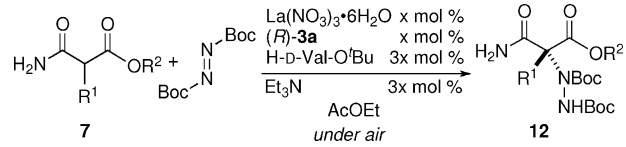


| | α-alkoxycarbonyl amide **7** | | | | | | | | |
|---|---|---|---|---|---|---|---|---|---|
| entry | $R^1$ | $R^2$ | | *x* | temp (°C) | product | time (h) | yield[b] (%) | ee (%) |
| 1 | Ph | Et | **7a** | 3 | rt | **12a** | 48 | 99 | 98 |
| 2[c] | 4-$FC_6H_4$ | Me | **7c** | 1 | rt | **12c** | 18 | >99 | 98 |
| 3[d] | 4-$FC_6H_4$ | Me | **7c** | 0.5 | rt | **12c** | 48 | 92[e] | 93 |
| 4 | 4-$CF_3C_6H_4$ | Et | **7e** | 1 | rt | **12e** | 13 | 90 | 96 |
| 5 | 4-$NO_2C_6H_4$ | Et | **7f** | 3 | 0 | **12f** | 13 | >99 | >99 |
| 6 | 3-thienyl | Et | **7j** | 3 | rt | **12j** | 13 | >99 | 93 |

[a] **7**: 0.2 mmol, BocN=NBoc: 0.24 mmol. [b] Isolated yield. [c] 0.4 mmol, BocN=NBoc: 0.48 mmol. [d] 0.8 mmol, BocN=NBoc: 0.96 mmol. [e] Determined by $^1H$ NMR with $Bn_2O$ as an internal standard.

group features of amide-based ligand **3a** were anticipated to be of prime importance for the association to form the ternary complex that engaged in the reaction. To probe this point, ester analogs of the ligand **3a** were synthesized and evaluated in the second-generation amination reaction of **1**. Both catechol analog (*S*)-**17** and salicyl ester analog (*S*)-**18** promoted the amination reaction of **1**, albeit with poor enantioselectivity, indicating that the amide functionality of (*R*)-**3a** was crucial for the formation of the ternary complex and/or recognition of **1**. Stronger coordination of a more Lewis basic amide carbonyl to $La^{3+}$ and/or hydrogen bonding of the N−H proton would be assumed to explain the preference of **3a** over **17** and **18** (Scheme 9). On the basis of the experimental results obtained above, a plausible catalytic cycle of the second-generation amination reaction is outlined in Figure 4. NMR and CD spectral analyses suggested that the catalyst components, $La(NO_3)_3$•$6H_2O$, (*R*)-**3a**, and H-D-Val-O'Bu in a 1:1:3 ratio, were in equilibrium between the associated and dissociated states in the reaction mixture with dissociated form predominating. ESI MS analysis and the linear relationship between enantiopurity of the catalyst and product enantioselectivity were in accord with the assumption that the catalytic asymmetric amination likely involves a monomeric

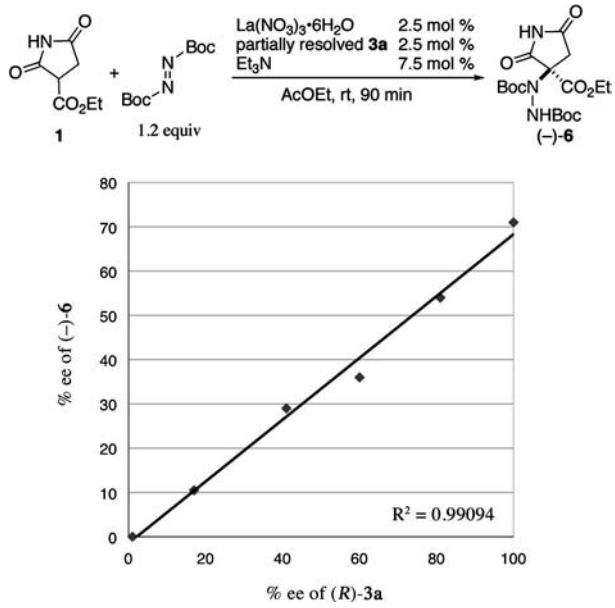


***Figure 3.*** Plot of % ee of product (−)-**6** versus % ee of ligand (*R*)-**3a** in the second-generation catalytic asymmetric amination using $Et_3N$ as a base.

***Scheme 9.*** Second-generation Catalytic Asymmetric Amination of **1** Using Ester Ligand (*S*)-**17** or (*S*)-**18**

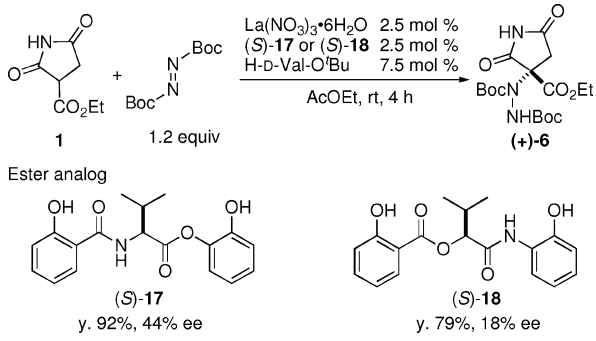


lanthanum complex such as **A**. The beneficial effects of salicylamide carbonyl over salicyl ester in the ligand substructure (Scheme 9) might be due to the higher Lewis basicity for coordination to $La^{3+}$ in a bidentate fashion. Subsequently, **7** was deprotonated by the complex **A** or H-D-Val-O*t*Bu, and the following coordination to $La^{3+}$ together with di-*tert*-butyl azodicarboxylate led to the transition structure **B**. Hydrogen bonding between (*R*)-**3a** and an enolate generated from **7**, amide NH (aminophenol side)/enolate oxygen, and the phenolic oxygen/imide N−H, may assist in determining the enantiofacial selection of the enolate.[43] The absolute stereochemistry of H-D-Val-O*t*Bu located in near proximity of $La^{3+}$ would contribute to direct azodicarboxylate approaching from Re-face of the enolate. An Eyring plot of the reaction provided large negative entropy of activation $\Delta S^{\ddagger} = -2.68 \times 10^2$ J mol$^{-1}$ K$^{-1}$, further supporting the notion that the association of catalyst components to form the ternary catalyst and an ordered transition state would be operative.[44] The nucleophilic addition from **B** followed by the protonation via $H^+$(H-D-Val-O*t*Bu)$NO_3^-$ afforded the desired product **12** and regenerated the monomeric lanthanum complex **A**, which was again in equilibrium with the dissociated state. It

(43) Bidentate coordination through two phenolic oxygens of (*R*)-**3a** was topologically unlikely.

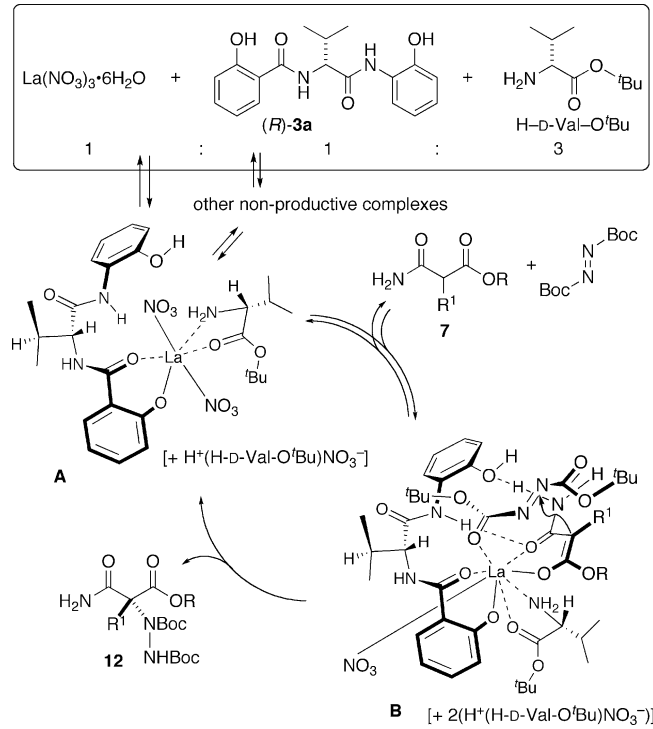


***Figure 4.*** Proposed catalytic cycle for second-generation catalytic asymmetric amination through ternary complex.

is intriguing that a metallic catalyst complex was in equilibrium between associated and dissociated forms while it exhibited an excellent enantioselection. Association of catalyst components and highly coordinative substrates through cooperative metal-coordination and hydrogen bonding enabled the employment of highly coordinative substrates in asymmetric catalysis.

## Conclusion

In summary, a catalytic asymmetric amination of nonprotected succinimide derivative **1** and α-alkoxycarbonyl amides **7** was developed with a lanthanum/amide-based ligand catalyst. These two classes of substrates share the same privileged structure likely recognized by the present catalytic system. The absence of precedents in the literature using these highly coordinative substrates in enantioselective catalysis highlights the utility of the lanthanum/amide-based ligand catalyst. Mechanistic studies using MS, NMR, CD analyses, and Eyring plot as well as several control and kinetic experiments suggested that the catalyst components were in equilibrium between the associated and dissociated state, and a ternary complex of La/(*R*)-**3a**/H-D-Val-O*t*Bu was likely involved. Cooperative coordination to $La^{3+}$ and hydrogen-bonding interactions were key to constructing the ternary complex and specific recognition/activation of highly coordinative nonprotected substrates **1** and **7**, affording the amination product in a highly enantioselective manner.

**Acknowledgment.** Financially support was provided by Grant-in-Aid for Scientific Research (S) (for M. S.) and Grant-in-Aid for Scientific Research on Innovative Areas (for N.K.) from JSPS and

(44) (a) Eyring, H. *J. Chem. Phys.* **1935**, *3*, 107. (b) Evans, M. G.; Polanyi, M. *Trans. Faraday Soc.* **1935**, *31*, 875. Usage of Eyring plot in asymmetric catalysis, see: (c) Josephsohn, N. S.; Kuntz, K. W.; Snapper, M. L.; Hoveyda, A. H. *J. Am. Chem. Soc.* **2001**, *123*, 11594. For experimental details, see Supporting Information.

MEXT. T.M. thanks JSPS for predoctoral fellowship. Drs. S. Furusho and A. Sato at JASCO international, and Dr. K. Konuma at JEOL Co. Ltd. are gratefully acknowledged for technical assistance in ESI MS analysis. We are grateful to Dr. M. Shiro at Rigaku Corporation for X-ray crystallographic analysis of compound (−)-**16**. We thank Prof. T. Ohwada and Dr. S. Uchiyama for assistance with the measurement of CD spectra of the catalysts.

**Supporting Information Available:** Experimental details and characterization of new compounds. Complete ref 30c. This material is available free of charge via the Internet at http://pubs.acs.org.

JA9052653